Reciprocity and behavioral heterogeneity govern the stability of social networks

Roslyn Dakin[1,2*] and T. Brandt Ryder[1,3§]

[1]Migratory Bird Center, Smithsonian Conservation Biology Institute, National Zoological Park, Washington, DC 20013, USA
[2]Department of Biology, Carleton University, Ottawa, ON, K1S 5B6, Canada
[3]Bird Conservancy of the Rockies, Fort Collins, Colorado, 80525, USA

Corresponding authors:
[*] roslyn.dakin@gmail.com
[§] ryder@si.edu

Abstract

The structure of social network interactions can determine the transmission of information, the spread of diseases, and the stability of diverse systems[1–6]. Despite this broad importance, a general framework for predicting social network stability has not been proposed[7,8]. Here, we use repeated measures of social structure in a cooperative bird species[9,10], the wire-tailed manakin, to evaluate the causes of temporal network stability. We find that social networks become destabilized when partners interact less frequently, and when social connectedness within the network increases. This negative effect of connectivity also predicts the temporal persistence of social partnerships on an annual timescale. These results were surprising[11], especially given that individuals who were more connected in the manakin population had more stable social partnerships. This apparent paradox arises from a within-individual behavioral trade-off between the maintenance of partner quantity and quality. Crucially, the trade-off is easily masked by substantial among-individual heterogeneity in sociality[12,13]. Using individual-based simulations, we show that these results are explained by a simple model that combines among-individual behavioral heterogeneity and reciprocity within the network. This model also demonstrates how among-individual heterogeneity, a ubiquitous feature of natural societies[13,14], can stabilize a social network. However, simulations including only heterogeneity or reciprocity alone were insufficient to generate the empirical patterns of stability. Together, these findings provide unifying principles that are expected to govern the stability of diverse social systems.

Social network structure – or, the way individuals are linked by repeated social interactions – can influence the transmission of information, culture, resources, and diseases[1–6]. Recent work has begun to demonstrate how changes to social network topology can have diverse costs[2,15–17] and benefits[18–20]. Theory is well established on the formation of biological networks and the resilience of ecological communities and gene co-expression systems to the loss of connections[14,21,22]. However, we lack a general framework to explain how behavioral processes within a social network govern the stability of partnerships[7,8]. A mechanistic understanding of these processes is essential to explain the diversity of network structures, predict the downstream fate of social interactions, and engineer societies.

Here, we combine repeated measures of social structure and mechanistic models to elucidate the drivers of social network stability in a cooperative system. Our empirical approach was based on autonomous biologging of a neotropical bird species, the wire-tailed manakin *Pipra filicauda*. Cooperative partnerships are a key part of the manakin social system[5,9,10], similar to humans[23]. Male wire-tailed manakins cooperate by forming display coalitions which are the basis of dynamic social networks[12,24]. Cooperation occurs at spatial locations known as leks, each of which typically has between 4-14 display territories and about twice as many males that visit the lek (each of whom limits his interactions to particular coalition partners[25]). The male-male coalitions that form at the lek territories are a prerequisite for an individual to attain territory ownership, and ultimately, sire offspring[9,10].

By tracking a population of 180 male manakins and 36,885 social interactions over three years, we took repeated measures of weighted social networks at 11 different lek sites (on average, repeated measures of the same lek were 21 days apart; IQR 17-24). To analyze the temporal dynamics of network topology from time t_1 to t_2, we define network stability as the number of male-male partnerships (network edges) shared by both time points divided by the number of partnerships at either time point (i.e., the intersection divided by the union; Fig. 1a). This metric captures the persistence of social partnerships at a collective scale, after accounting for any changes in the representation of particular individuals (nodes)[26]. We found that the manakin social networks were more stable than expected by chance (Fig. 1a), similar to other social animals[15,27,28]. However, stability was not constant, because each network fluctuated across a range of values (mean stability 0.43 ± SD 0.23; repeatability of stability 0, 95% CI 0–0.22).

To test how the social structure at t_1 might predict subsequent network stability, we used a mixed-effects modelling framework. We found that three properties of the social network structure could explain 28% of the variation in network stability in the best-fit statistical model: network size (the number of individuals or nodes in the network), network weight (the average frequency of social interactions), and network density (the proportion of possible partnerships that actually occurred, which is a measure of connectivity; Fig. 1b–d). Our analysis also controlled for the timing (year and mean Julian date) when each sample of a network was taken. All else being equal, when more individuals within the network interacted (greater connectivity), and when dyads in the network interacted less frequently, the social structure destabilized over the subsequent weeks (Fig. 2 and Extended Data Tables 1-2).

The result that network connectivity decreases stability was unexpected, given that connectedness is thought to foster social cohesion[11]. To provide a mechanistic explanation for these results, we built a simulation model based on the hypothesis that individual behaviors would drive emergent properties of the network[14]. Our individual-based model assumed simple rules that describe a scenario of reciprocity[23] with among-individual heterogeneity[13,14]: (i) social

partnerships are formed through reciprocal partner choice, wherein both individuals must choose each other; (ii) individuals prefer social partners with whom they have interacted in the recent past[29]; and (iii) individuals differ in the expression of behavioral phenotype (sometimes referred to as among-individual heterogeneity, or personality). This third assumption of heterogeneity has been found to be ubiquitous in humans and animals[13] and has been shown to influence collective performance[30] and the evolution of cooperation[31,32]. We generated 3,000 initial networks *de novo* across a broad range of network sizes, weights, and densities, and used these initial random networks to parameterize (ii) and (iii). We then allowed the individual nodes to interact repeatedly. Finally, we computed the stability of each network, by comparing the initial structure to the one that resulted from the newly-simulated interactions.

Similar to the manakin data, we found that well-connected networks (high density) with low frequency of cooperation (low weight) were less stable (Fig. 2). Hence, the simple model of reciprocity plus heterogeneity was sufficient to recreate patterns of temporal change observed in the empirical networks. Moreover, we found that null model simulations lacking all three assumptions (i–iii), or that included only (i), (ii), or (iii) alone, were insufficient to generate the empirical patterns of stability. In null models that lacked reciprocity, denser networks were also consistently more stable, making the negative effect in the empirical data particularly striking. Overall. our findings indicate that both behavioral processes, reciprocity and heterogeneity, are necessary to recreate the weight and density effects. Finally, we found that the larger simulated networks with more individuals were also significantly less stable, independent of network weight and density. This effect of network size was also consistent with the manakin data (although in the empirical analysis, it was not quite statistically significant; see Extended Data Table 3).

Why are some social partnerships able to persist through time[15,28]? To understand how social structure might influence the fidelity of particular bonds over longer timescales, we analyzed the annual persistence of 669 manakin partnerships from one season to the next (Fig. 3a–b). The analysis accounted for the identities of the partners, the year, the lek network where the partnership occurred, and other factors including the spatial overlap of the individuals. Two features predominantly explained the variation in partnership persistence: the interaction frequency (edge weight), and the local social density (edge connectivity, which quantifies the number of alternative paths that can connect two partners in a social network). Specifically, a partnership was more likely to persist if the two individuals interacted more frequently, but had lower connectivity in their social neighborhood. These results are consistent with the phenomena observed at the network level over shorter weekly timescales (Fig. 2). Moreover, we found that the simulation of reciprocity and heterogeneity could also recreate our empirical results on partnership persistence (Fig. 3c–d).

These negative effects of social connectivity suggest that social stability is governed by a fundamental trade-off between the quantity and quality of social partnerships. Contrary to the trade-off hypothesis, however, the manakins with more partners (i.e., those with higher average degree centrality) formed coalitions that were more likely to persist through time (Fig. 4a). This apparent paradox is resolved by partitioning the variation among- and within-individuals (Fig. 4b-c). Among individuals, the males who were more connected were better able to maintain their partnerships (Fig. 4b). However, when a given male had more partners than his average, he was less able to maintain them (Fig. 4c). Thus, each individual may have a different threshold for the number of stable coalition partnerships he is able to maintain. This explains why densely connected social networks are less stable (Fig. 2) even though well-connected individuals are

better at maintaining partnerships (Fig. 4a-b). In wire-tailed manakins, the proximate causes of this among-individual heterogeneity are not yet well understood[33], but hypotheses for future study may include a male's quality, social experience, and/or his compatibility with his partners. An important conclusion from our results is that among-individual heterogeneity can often mask behavioral trade-offs[13], including in humans, emphasizing the importance of longitudinal studies.

How might the magnitude of behavioral heterogeneity influence the stability of cooperative networks[30]? Our simulation model provided an opportunity to explore this question. To measure heterogeneity, we computed the coefficient of variation in degree centrality (CV_{degree}) in each of the initial networks; higher values indicate greater behavioral heterogeneity in the system[21]. We found that CV_{degree} had a significant positive effect on subsequent network stability (Fig. 5), demonstrating that individual variation in sociality can foster stable social networks. This is similar to the way some ecological systems are affected by heterogeneity (e.g., CV of connectedness (degree) and edge weights)[21,22]. In social systems, behavioral heterogeneity can also include suites of correlated traits such as dispersal, risk-taking, and cognitive ability, in addition to variation in sociality[7,13,34]. Further study is needed to understand how this covariation influences social network stability and the evolution of complex social behavior.

In human societies, social media platforms are rapidly transforming our social networks by increasing the density of online relationships at a potential cost to face-to-face interactions[6,35]. Here, we show how these changes can broadly destabilize emergent social structure. Our results explain why increased connectedness is detrimental for the stability and maintenance of cooperative networks. When individuals become too connected, time and energy constraints can limit the ability to reciprocate social partnerships. An important question is how much topological changes affect other dynamics, such as the spread of emotions, cultural evolution, and disease transmission. Although our study focused on one type of cooperative system, many other social networks are formed as a result of competitive, aggressive, mating, and information-sharing interactions[7]. As a unifying framework, we propose that social stability in these other contexts will also be determined by the simple behavioral processes that generate heterogeneity, partner preferences, and the symmetry of partner choice.

METHODS

Field methods

Observed social networks were based on a study of wire-tailed manakins, *Pipra filicauda*, at the Tiputini Biodiversity Station in Ecuador (0º 38' S, 76º 08' W, 200 m elevation). Male wire-tailed manakins perform cooperative courtship displays at exploded leks, where males are in acoustic but not visual contact[36]. The population at Tiputini has been monitored since 2002 to study the fitness benefits of cooperative behavior[9,10]. The present study spanned three field seasons (December-March) in 2015-16, 2016-17 and 2017-18, and used an automated proximity data-logging system to record cooperative interactions among males, as described in previous protocols that provide detailed algorithms[12,24]. Briefly, manakins were captured using mist-nets and each male was outfitted with unique color bands and a coded nano-tag transmitter (NTQB-2, Lotek Wireless; 0.35 g). To record the social network at a given lek, proximity data-loggers (SRX-DL800, Lotek Wireless) were deployed in each territory to record all tag detections within the territory from 06:00 to 16:00 for ~6 consecutive days (± SD 1 day)[12,33]. Because the social interactions were measured using this automated system, the networks were constructed blind to the sociality of particular individuals and/or leks. Territory ownership was assigned using direct

observation of color-banded males at the display sites[9], and was subsequently verified in the proximity data. Sample sizes were not predetermined because our aim was to track all individuals within the studied leks[33]. All animal research was approved by the Smithsonian ACUC (protocols #12-23, 14-25, and 17-11) and the Ecuadorean Ministry of the Environment (MAE-DNB-CM-2015-0008).

Data processing

All data processing and statistical analyses were performed in R 3.5.1[37]. Male-male cooperative interactions on the display territories were determined using spatiotemporal overlap of tag detections in the proximity data (see our previous study[12] for detailed algorithms and ground-truthing data). We used these dyadic interactions to build a weighted social network for each lek recording session, with nodes representing male identities, and the edges weighted by the frequency of dyadic interactions summed over the recording session. In total, we characterized 86 repeated measures of the social networks at 11 leks (mean 7.8 sessions per lek, ± SD 3.7) from 29,760 sampling session hours and 36,885 unique social interactions among 180 individuals. We used a clustering analyses in the igraph package[38,39] to verify that our sampling design was well-matched to the inherent social structure of the population (Extended Data Fig. 1).

Network stability

The stability of social network topology is determined by both the gain and loss of associations over time. We therefore defined a bidirectional metric of social network stability that compares two repeated measurements of a social network structure, N, at times t_1 and t_2. The stability of N over the period $t_1 \leftrightarrow t_2$ is defined as the number of social partnerships (i.e., edges) shared by N_1 and N_2 (i.e., intersection $\cap$), divided by the total number of unique edge connections in either N_1 or N_2 (i.e., union $\cup$). Using E to represent network edges, stability is thus defined as:

$$Stability = \frac{(E_1 \cap E_2)}{(E_1 \cup E_2)}$$

In most social networks, individuals (or nodes) can also be gained or lost over time, which alters the set of possible interactions that could occur. To ensure that our measure of social network stability was based on edges that could have occurred at both time points, only individuals who were present at both t_1 and t_2 were included in the calculation[26]. Therefore, our definition captures stability of the network topology after accounting for changes in the presence of individual nodes. To further account for measurement error[40], we also filtered the stability calculation to include only significant edges that met two criteria in our empirical data: (1) they occurred more often than the average occurrence in 1,000 random permutations of the interaction data, and (2) they occurred at least six times during the recording session (i.e., on average, about once per day). The second criterion ensured that rare interactions were not easily deemed significant. The value of six was chosen to correspond to the average length of the recording sessions, but we also verified that other thresholds >2 did not influence our results.

The average stability score for the manakin networks was 0.43 (± SD 0.23, n = 60 networks at 11 leks). Note that the sample size of 60 is smaller than the total number of recording sessions, because the stability dataset is limited to networks that were also sampled at t_2 within the same season. The observed networks were also more stable than expected by chance (paired t-test, $t = 12.08$, $p < 0.0001$), as determined by random network rewiring (100 edge

permutations for each of the 60 measurements; grand mean null expected stability 0.07 ± SD 0.05).

Network-level analyses

To determine how network-level properties at t_1 predict subsequent network stability, we fit mixed-effects regression models using the package lme4[41] (n = 60 networks at 11 leks). The analysis included lek identity as a random effect, and to account for potential temporal trends, we also included field season (categorial) and mean Julian date of the social interactions (continuous) as two fixed effects. We considered five other fixed-effects that characterize the network structure: (1) network weight, a measure of the average relationship frequency, calculated as the mean of the log-transformed edge weights; (2) network density, a measure of connectivity calculated as the proportion of relationships that actually occurred relative to a completely connected network; (3) network transitivity, a measure of the probability that a given individual/node's social partners are also connected; and (4) network modularity, a measure of how well the network can be subdivided into separate communities using the random-walk algorithm[38,39]. To account for the fact that network-level properties often scale with network size[14,42] (Fig. 1e–g), we also included (5) the log-transformed number of individuals/nodes in the social network. Because density, transitivity, and modularity were all similar measures of network connectivity, and because the sample size was relatively small, we used a model selection procedure to compare candidate models that included either (2), (3) or (4), and/or (1), or none of (1)-(4); full results are provided in Extended Data Tables 1-2. Finally, we evaluated whether our measures of network stability were influenced by two logistical factors: first, sampling effort, and second, a testosterone manipulation experiment that was conducted for a separate study in 2016-17 and 2017-18 (n = 9 individuals out of 180 that were implanted with testosterone[33]). To verify that these two logistical factors did not influence our results, we added additional fixed effects for the number of recording hours (median 75, mean 73 ± SD 10) and/or the number of hormone-manipulated individuals in a given network (median 0, mean 0.10 ± SD 0.41), neither of which had a significant effect on network stability (all $p > 0.43$). We also verified that all conclusions of our network-level analysis were unchanged when accounting for either or both of these covariates. To determine the repeatability of network properties of the leks, we calculated the proportion of total variation that was due to differences among the leks using mixed-effects models with lek as the random effect and field season and Julian date as fixed effects[41,43].

Edge-level analysis

The edge-level analysis examined the persistence of manakin social partnerships on an annual timescale. This analysis considered 669 dyadic partnerships among 91 individuals wherein both individuals in the partnership were also present and tagged in the subsequent breeding season. The binary response variable, partnership persistence, was defined as whether a partnership was both sustained and significant in the subsequent season (see Network stability for criteria for significance). Because both individuals in a social partnership can contribute to its fate, and because they both had other partnerships in the dataset, we modelled persistence using a multiple-membership structure in a binomial mixed-effects regression model, fit with the brms package[44]. This method can be used to account for multiple partner identities within a single random effect structure[12,44–46]. In our analysis, the two identities were weighted equally, because we assumed they could both determine partnership persistence. An additional random effect was

included to account for the lek where each partnership occurred. The analysis also included three fixed effects to account for the initial field season (categorical), the territorial status of the pair (categorical; either two territory-holders, a territory holder plus a floater, or two floaters[9]), and the initial spatial overlap of the pair, which can influence the probability of interaction[28]. Because manakins use discrete display territories, we defined the spatial overlap of two males as the log-inverse of the chi-squared statistic comparing their distributions of territory detections (pings) in the proximity data; larger values of this metric indicate greater spatial overlap. To test our main hypothesis that edge-level network properties would predict partnership persistence, we also included the following fixed effects: (1) edge weight, or the log-transformed social interaction frequency; (2) edge betweenness, a measure of social centrality, defined as the log-transformed number of shortest paths passing through that edge; and (3) edge connectivity, a measure of social density, defined as the minimum number of edges that must be removed to eliminate all paths between the two individuals/nodes in a partnership[39]. We ran four independently seeded chains with default priors, storing 2,000 samples from each chain, and verifying that the convergence statistics were all equal to one[44] (Extended Data Table 4).

Among-individual analysis

To test whether partnership persistence could be attributed to behavioral differences among individual manakins, we refit the analysis described above, but without accounting for (1)-(3) listed above. The random intercepts from this model provide an estimate of among-individual variation in social stability[12,43]. We hypothesized that the following behavioral phenotypes[12] could affect this trait: (1) a male's average daily effort, measured using his log-transformed count of detections (pings) on the leks; (2) his average daily strength, using his log-transformed sum of interaction frequencies; (3) his average daily degree, using his log-transformed number of social partnerships, and (4) and his average daily social importance, defined as the exclusivity of his partnerships (see our previous protocol[12] for additional details). Because these four phenotypes were also correlated[12,33], we compared six candidate regression models, four of which included only one behavioral phenotype, one of which included all four phenotypes, and one that included no behavioral phenotypes (n = 91 individuals; see Extended Data Table 5). All candidate models included a male's status as either a territory-holder or floater.

Quantity-quality trade-off analysis

We next sought to test the hypothesis that individuals in a network face a trade-off between the quantity (number of partners) and stability of those social partnerships. Because among-individual variance can mask trade-offs that occur within-individuals[47], testing this hypothesis requires a variance-partitioning approach. To achieve this, we defined repeated measures of individual partnership maintenance as the proportion of a male's coalition partners that were maintained from a given recording session to the next recording session (n = 565 repeated measures of 152 individuals). Note that a male had to be present, tagged, detected, and not part of the hormone manipulation experiment in both the initial and subsequent recording sessions to be included in this sample. We used within-group centering to partition the variation in the predictor variable, degree centrality, within- and among-individuals[48]. The first step was to determine log-transformed degree for each male in each recording session; next, we took a single average value per male; and finally, we calculated relative degree in each recording session as a male's log-transformed degree minus his overall average. Thus, average and relative degree represent two orthogonal predictors that can be analyzed within the same regression model. The

analysis was fit as a binomial mixed-effects model in lme4[41] with a random effect of individual identity, and it also included two categorical fixed effects to account for field season and territorial status (Extended Data Table 6).

Individual-based simulation models

To provide a mechanistic explanation for how individual behavior scales up to influence social network stability, we developed a simple individual-based simulation model. The model was based on the general principles of social reciprocity[23] and among-individual behavioral heterogeneity. There were three core assumptions: (i) individuals had to actively choose each other in order to form a partnership; (ii) each individual had a ranked set of preferences for social partners, predicted by its previous social interaction frequencies, and (iii) individuals express consistent differences in their social behavior (referred to as behavioral phenotype). The second rule (ii) is supported by strong evidence that social relationships are non-random and persist over long time-scales in human and nonhuman animals[15,28]. Together, (i) and (ii) also represent a form of reciprocal altruism[23], because prior interactions increase the probability that a partner will be re-chosen. Rule (iii) represents a phenomenon that is often referred to as among-individual variation, heterogeneity, or personality; it has empirical support across vertebrates[13], including in manakins[12].

To experimentally test the effects of network size, weight, and density on network stability, we generated 3,000 initial networks with diverse properties that were within the range of the observed data. Network size was first chosen from the range of 11-20 individuals or nodes (10 size bins). To manipulate network density along the same range observed in the manakin data, we first generated completely connected networks, and then randomly removed edges until a target initial density was achieved (targets ranging from 0.2-0.8, for a total of 20 target density bins). To generate a broad range of initial network weights, each edge weight was first sampled from the manakin data, and then multiplied by a weight constant ranging from 0.2-2.0 (15 weight factor bins). The resulting edge weights were then rounded up, to a maximum of 500. We generated 3,000 networks with all possible combinations of these network properties (10 x 15 x 20 = 3,000).

The simulation proceeded as follows. First, to satisfy rule (ii), we assigned a set of preferences to each node based on that node's partnerships in the initial starting network. The set of preferences included all other nodes, ranked by interaction frequency with the focal node in the initial network. Hence, the probability of choice was correlated with initial interaction frequency. To satisfy rule (iii), each node was also allotted a specific number of interaction attempts per time step (ranging from 1-4). This number was calculated by log-transforming the strength of the focal node in the initial network (also referred to as weighted degree) to obtain its behavioral phenotype; higher values meant that a node could attempt more social interactions per unit time. To satisfy rule (i), a partnership was only formed if both nodes chose each other within a given time step. The simulation ran over five time steps and the final network was determined by summing the new interactions that occurred (Extended Data Fig. 2). No filtering was applied to calculate network stability in the simulation. For the null model, we followed the same procedures above, except that each individual's partner choice probabilities were assigned randomly to the set of all other nodes, the number of attempted interactions per time step was fixed across individuals, and reciprocal partner choice was not required for partnership formation in the null model (i.e., assumptions ii, iii, and i were removed). We also tested models with either (i), (ii), or (iii) alone. After running the simulations, we used linear models to statistically

analyze the variation in network stability and examine our three predictors of interest: network size, weight, and density. To compare the results of this analysis with the statistical estimates derived from the observed data, all predictors and response variables were standardized to have a mean of 0 and SD of 1 (Extended Data Table 3). To test whether the simulation model of reciprocity and heterogeneity could also explain our edge-level analysis, we used a binomial mixed-effects regression of edge persistence in the simulation, with the identity of the initial network as a random effect, and edge weight and edge connectivity as the predictors.

Data availability

The data and R code necessary to reproduce our results are available at: https://figshare.com/s/470aeac186a9dab72860

References

1. Watts, D. J. & Strogatz, S. H. Collective dynamics of 'small-world' networks. *Nature* **393**, 440 (1998).
2. Flack, J. C., Girvan, M., Waal, F. B. M. de & Krakauer, D. C. Policing stabilizes construction of social niches in primates. *Nature* **439**, 426 (2006).
3. Aplin L. M., Farine D. R., Morand-Ferron J. & Sheldon B. C. Social networks predict patch discovery in a wild population of songbirds. *Proc. R. Soc. B Biol. Sci.* **279**, 4199–4205 (2012).
4. Hoyt, J. R. *et al.* Cryptic connections illuminate pathogen transmission within community networks. *Nature* **563**, 710 (2018).
5. McDonald, D. B. Predicting fate from early connectivity in a social network. *Proc. Natl. Acad. Sci.* **104**, 10910–10914 (2007).
6. Christakis, N. A. & Fowler, J. H. *Connected: The surprising power of our social networks and how they shape our lives.* (Little, Brown and Company, 2009).
7. Sih, A., Hanser, S. F. & McHugh, K. A. Social network theory: new insights and issues for behavioral ecologists. *Behav. Ecol. Sociobiol.* **63**, 975–988 (2009).
8. Pinter-Wollman, N. *et al.* The dynamics of animal social networks: analytical, conceptual, and theoretical advances. *Behav. Ecol.* **25**, 242–255 (2014).

9. Ryder, T. B., McDonald, D. B., Blake, J. G., Parker, P. G. & Loiselle, B. A. Social networks in the lek-mating wire-tailed manakin (*Pipra filicauda*). *Proc. R. Soc. B* **275**, 1367–1374 (2008).

10. Ryder, T. B., Parker, P. G., Blake, J. G. & Loiselle, B. A. It takes two to tango: reproductive skew and social correlates of male mating success in a lek-breeding bird. *Proc. R. Soc. B* **276**, 2377–2384 (2009).

11. Brent, L. J. N. Friends of friends: are indirect connections in social networks important to animal behaviour? *Anim. Behav.* **103**, 211–222 (2015).

12. Dakin, R. & Ryder, T. B. Dynamic network partnerships and social contagion drive cooperation. *Proc. R. Soc. B Biol. Sci.* **285**, 20181973 (2018).

13. Bell, A. M., Hankison, S. J. & Laskowski, K. L. The repeatability of behaviour: a meta-analysis. *Anim. Behav.* **77**, 771–783 (2009).

14. Barabási, A.-L. & Albert, R. Emergence of scaling in random networks. *Science* **286**, 509–512 (1999).

15. Silk, J. B. *et al.* Strong and consistent social bonds enhance the longevity of female baboons. *Curr. Biol.* **20**, 1359–1361 (2010).

16. Laskowski, K. L., Montiglio, P.-O. & Pruitt, J. N. Individual and group performance suffers from social niche disruption. *Am. Nat.* **187**, 776–785 (2016).

17. Brent, L. J. N., Ruiz-Lambides, A. & Platt, M. L. Family network size and survival across the lifespan of female macaques. *Proc. R. Soc. B Biol. Sci.* **284**, 20170515 (2017).

18. Fehl, K., Post, D. J. van der & Semmann, D. Co-evolution of behaviour and social network structure promotes human cooperation. *Ecol. Lett.* **14**, 546–551 (2011).

406 19. Rand, D. G., Arbesman, S. & Christakis, N. A. Dynamic social networks promote cooperation in experiments with humans. *Proc. Natl. Acad. Sci.* **108**, 19193–19198 (2011).

408 20. Stroeymeyt, N. *et al.* Social network plasticity decreases disease transmission in a eusocial insect. *Science* **362**, 941–945 (2018).

410 21. Gross, T., Rudolf, L., Levin, S. A. & Dieckmann, U. Generalized models reveal stabilizing factors in food webs. *Science* **325**, 747–750 (2009).

412 22. Gao, J., Barzel, B. & Barabási, A.-L. Universal resilience patterns in complex networks. *Nature* **530**, 307–312 (2016).

414 23. Trivers, R. L. The evolution of reciprocal altruism. *Q. Rev. Biol.* **46**, 35–57 (1971).

24. Ryder, T. B., Horton, B. M., Tillaart, M. van den, Morales, J. D. D. & Moore, I. T. Proximity

416 data-loggers increase the quantity and quality of social network data. *Biol. Lett.* **8**, 917–920 (2012).

418 25. Ryder, T. B., Blake, J. G., Parker, P. G. & Loiselle, B. A. The composition, stability, and kinship of reproductive coalitions in a lekking bird. *Behav. Ecol.* **22**, 282–290 (2011).

420 26. Poisot, T., Canard, E., Mouillot, D., Mouquet, N. & Gravel, D. The dissimilarity of species interaction networks. *Ecol. Lett.* **15**, 1353–1361 (2012).

422 27. Baird, R. W. & Whitehead, H. Social organization of mammal-eating killer whales: group stability and dispersal patterns. *Can. J. Zool.* **78**, 2096–2105 (2000).

424 28. Shizuka, D. *et al.* Across-year social stability shapes network structure in wintering migrant sparrows. *Ecol. Lett.* **17**, 998–1007 (2014).

426 29. Croft, D. P. *et al.* Social structure and co-operative interactions in a wild population of guppies (*Poecilia reticulata*). *Behav. Ecol. Sociobiol.* **59**, 644–650 (2006).

30. Pruitt, J. N., Bolnick, D. I., Sih, A., DiRienzo, N. & Pinter-Wollman, N. Behavioural hypervolumes of spider communities predict community performance and disbandment. *Proc. R. Soc. B Biol. Sci.* **283**, 20161409 (2016).

31. Perc, M. & Szolnoki, A. Social diversity and promotion of cooperation in the spatial prisoner's dilemma game. *Phys. Rev. E* **77**, 011904 (2008).

32. Santos, F. C., Pinheiro, F. L., Lenaerts, T. & Pacheco, J. M. The role of diversity in the evolution of cooperation. *J. Theor. Biol.* **299**, 88–96 (2012).

33. Ryder, T. B., Roslyn Dakin, Vernasco, B. J., Horton, B. M. & Moore, I. T. Testosterone drives status-specific patterns of cooperation in a social network. Preprint. https://doi.org/10.1101/453548. (preprint in review). doi:https://doi.org/10.1101/453548

34. Sih, A., Bell, A. & Johnson, J. C. Behavioral syndromes: an ecological and evolutionary overview. *Trends Ecol. Evol.* **19**, 372–378 (2004).

35. Oberst, U., Wegmann, E., Stodt, B., Brand, M. & Chamarro, A. Negative consequences from heavy social networking in adolescents: The mediating role of fear of missing out. *J. Adolesc.* **55**, 51–60 (2017).

36. Hoglund, J. & Alatalo, R. V. *Leks*. (Princeton University Press, 1995).

37. R Core Team. *R 3.5.1: A Language and Environment for Statistical Computing*. (R Foundation for Statistical Computing, 2018).

38. Pons, P. & Latapy, M. Computing communities in large networks using random walks. **10**, 191–218 (2006).

39. Csardi, G. & coathors. *igraph 1.2.2: network analysis and visualization.* (2018).

40. Farine, D. R., Freckleton, R. & Rands, S. A guide to null models for animal social network analysis. *Methods Ecol. Evol.* **8**, 1309–1320 (2017).

41. Bates, D. *et al. lme4 1.1-17: linear mixed-effects models using 'Eigen' and S4*. (2018).

42. Thébault, E. & Fontaine, C. Stability of ecological communities and the architecture of mutualistic and trophic networks. *Science* **329**, 853–856 (2010).

43. Nakagawa, S. & Schielzeth, H. Repeatability for Gaussian and non-Gaussian data: a practical guide for biologists. *Biol. Rev.* **85**, 935–956 (2010).

44. Buerkner, P.-C. *brms 2.5.0: Bayesian regression models using Stan*. (2018).

45. Buerkner, P.-C. brms: an R package for Bayesian multilevel models Using Stan. *J. Stat. Softw.* **80**, (2017).

46. Browne, W. J., Goldstein, H. & Rasbash, J. Multiple membership multiple classification (MMMC) models. *Stat. Model.* **1**, 103–124 (2001).

47. van Noordwijk, A. J. & de Jong, G. Acquisition and allocation of resources: Their influence on variation in life history tactics. *Am. Nat.* **128**, 137–142 (1986).

48. van de Pol, M. & Wright, J. A simple method for distinguishing within- versus between-subject effects using mixed models. *Anim. Behav.* **77**, 753–758 (2009).

Supplementary Information

Extended Data Figures 1-2 and Tables 1-6

Acknowledgements

We thank Ben Vernasco, Camilo Alfonso, Brent Horton, Ignacio Moore, Brian Evans, David and Consuelo Romo, Kelly Swing, Diego Mosquera, Gabriela Vinueza, the Tiputini Biodiversity Station of the Universidad San Francisco de Quito, and Julie Morand-Ferron. Funding was provided by National Science Foundation (NSF) IOS 1353085 and the Smithsonian Migratory Bird Center.

Author Contributions

RD and TBR designed the study, analyzed the data, and wrote the paper. TBR collected the data. RD wrote the simulations.

Data Deposition

The data and R code necessary to reproduce our results are available at: https://figshare.com/s/470aeac186a9dab72860

Competing Interests

We declare no competing interests.

FIGURE LEGENDS

Fig. 1. The temporal stability of social networks. a, Variation in network structure is generated by the temporal dynamics of social interactions. In **a**, two initial manakin networks are shown (blue and green), with individuals depicted as nodes, and edge thickness weighted by the interaction frequency on a log scale. When the same two networks were sampled a second time, the edge structure of the blue network remained mostly stable, whereas the structure of the green network had largely changed. Social networks in wire-tailed manakins were more stable than expected by chance, as shown by the fact that nearly all of the observed stabilities in the grey distribution exceed the 95% confidence interval of the null expectation (vertical black bar; the null is based on an edge permutation). The observed networks also varied in properties such as: **b**, the number of individuals (size), **c**, the proportion of possible relationships that occurred (density), and **d**, the average frequency of interactions (weight). The illustrated networks in **b–d** are colored according to the gradients along the x-axes. In the illustration for network weight, edge thicknesses are also scaled to the average interaction frequency. **e–f**, Scaling of density and weight with network size. **g**, Repeatability of network properties ±95% confidence intervals (n = 86 repeated measures, 60 for stability, of 11 lek networks).

Fig. 2. A model of reciprocity and behavioral heterogeneity predicts network stability. a–b, The stability of a social network is positively associated with the average frequency of interactions (weight), whereas stability is negatively associated with the proportion of possible relationships that occurred (density). These effects were confirmed in an individual-based simulation of reciprocity that combined three behavioral rules: (i) a requirement for reciprocal partner choice, (ii) a preference for previous partners, and (iii) repeatable variation among individuals in social behavior. The sample sizes are n = 60 repeated measures of 11 lek networks in the observed data, and n = 3,000 simulated networks. Note that the standardized coefficients derived from the simulation fall within the shaded 95% confidence intervals of the observed data, unlike the null model. The 95% confidence intervals for all simulation estimates are not visible because they are narrower than the data points. The right columns in **a** and **b** show partial residual plots from the statistical analyses, after accounting for additional covariates (Extended Data Tables 1-3). For clarity, shading is used to show the 95% central range for partial residuals binned along the x-axis, instead of plotting all 3,000 data points for the simulations.

Fig. 3. Social structure predicts the long-term persistence of social partnerships. a–b, The probability that a partnership persisted across years was greater when the two partners interacted at a higher frequency (edge weight), but had fewer paths connecting them in the social network (edge connectivity). Data points show how edge weight and connectivity (x-axes) determine the predicted probability of partnership persistence (y-axis) in a multiple-membership analysis (n = 669 partnerships among 91 individuals). **c–d,** The influence of edge weight and connectivity is also found in the individual-based model of reciprocity described in Fig. 2. Shaded areas in **c–d** show the 95% central range for partial residuals binned along the x-axis.

Fig. 4. Behavioral heterogeneity and social stability. Social behavior varies both within and among individuals. **a,** At the among-individual level, manakins who were consistently more gregarious fostered greater long-term social stability. The plot in **a** shows how an individual's behavior (x-axis) predicts his effect on annual partnership persistence (y-axis, ±95% confidence

interval of the prediction line). Males who consistently interacted with more partners per day (high average daily degree) promoted long-term coalition persistence (n = 90 individuals). **b–c**, A trade-off is revealed when examining repeated measures within-individuals. The plots in **b** and **c** show partial residuals from a variance partitioning analysis of within-season partnership (or edge) maintenance (n = 565 repeated measures of 152 individuals). Despite the positive among-individual effect shown in **b**, at times when a given male had more partners than his average in **c**, he was less able to maintain stable partnerships. To visualize among- and within-individual variation, a single average is plotted for each male in **b** (± SE if a male had >3 measurements), whereas a separate linear fit is shown for individuals with >3 measurements in **c**. **d,** Social networks with greater among-individual behavioral heterogeneity (CV_{degree}) were also more temporally stable in an individual-based simulation. The y-axis shows partial residuals from an analysis that also accounts for the effects of network size, weight, and density (n = 3,000). Shading indicates the 95% central range for partial residuals binned along the x-axis.

Figure 1

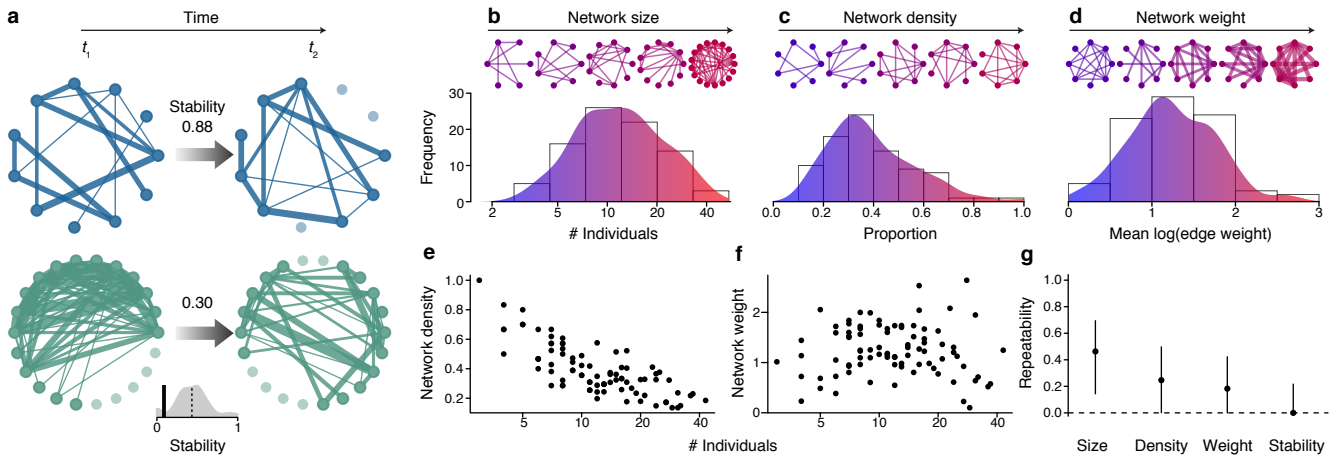

Fig. 1. The temporal stability of social networks. a, Variation in network structure is generated by the temporal dynamics of social interactions. In a, two initial manakin networks are shown (blue and green), with individuals depicted as nodes, and edge thickness weighted by the interaction frequency on a log scale. When the same two networks were sampled a second time, the edge structure of the blue network remained mostly stable, whereas the structure of the green network had largely changed. Social networks in wire-tailed manakins were more stable than expected by chance, as shown by the fact that nearly all of the observed stabilities in the grey distribution exceed the 95% confidence interval of the null expectation (vertical black bar; the null is based on an edge permutation). The observed networks also varied in properties such as: b, the number of individuals (size), c, the proportion of possible relationships that occurred (density), and d, the average frequency of interactions (weight). The illustrated networks in b–d are colored according to the gradients along the x-axes. In the illustration for network weight, edge thicknesses are also scaled to the average interaction frequency. e–f, Scaling of density and weight with network size. g, Repeatability of network properties ±95% confidence intervals (n = 86 repeated measures, 60 for stability, of 11 lek networks).

Figure 2

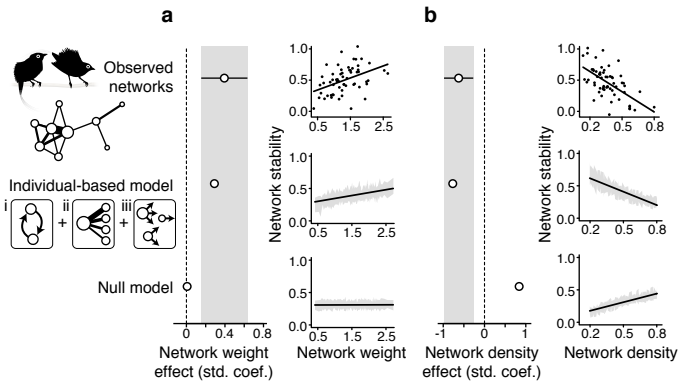

Fig. 2. A model of reciprocity and behavioral heterogeneity predicts network stability. a–b, The stability of a social network is positively associated with the average frequency of interactions (weight), whereas stability is negatively associated with the proportion of possible relationships that occurred (density). These effects were confirmed in an individual-based simulation of reciprocity that combined three behavioral rules: (i) a requirement for reciprocal partner choice, (ii) a preference for previous partners, and (iii) repeatable variation among individuals in social behavior. The sample sizes are n = 60 repeated measures of 11 lek networks in the observed data, and n = 3,000 simulated networks. Note that the standardized coefficients derived from the simulation fall within the shaded 95% confidence intervals of the observed data, unlike the null model. The 95% confidence intervals for all simulation estimates are not visible because they are narrower than the data points. The right columns in a and b show partial residual plots from the statistical analyses, after accounting for additional covariates (Extended Data Tables 1-3). For clarity, shading is used to show the 95% central range for partial residuals binned along the x-axis, instead of plotting all 3,000 data points for the simulations.

Figure 3

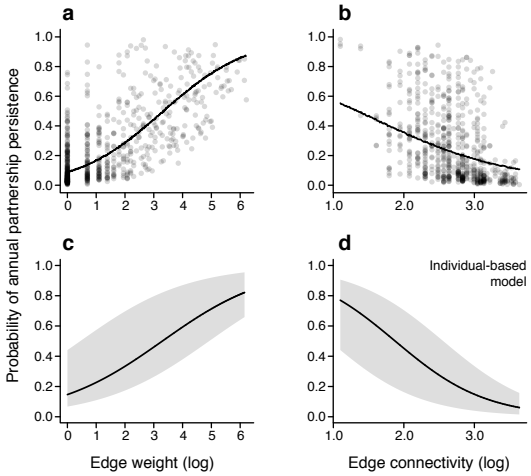

Fig. 3. Social structure predicts the long-term persistence of social partnerships. a–b, The probability that a partnership persisted across years was greater when the two partners interacted at a higher frequency (edge weight), but had fewer paths connecting them in the social network (edge connectivity). Data points show how edge weight and connectivity (x-axes) determine the predicted probability of partnership persistence (y-axis) in a multiple-membership analysis (n = 669 partnerships among 91 individuals). c–d, The influence of edge weight and connectivity is also found in the individual-based model of reciprocity described in Fig. 2. Shaded areas in c–d show the 95% central range for partial residuals binned along the x-axis.

Figure 4

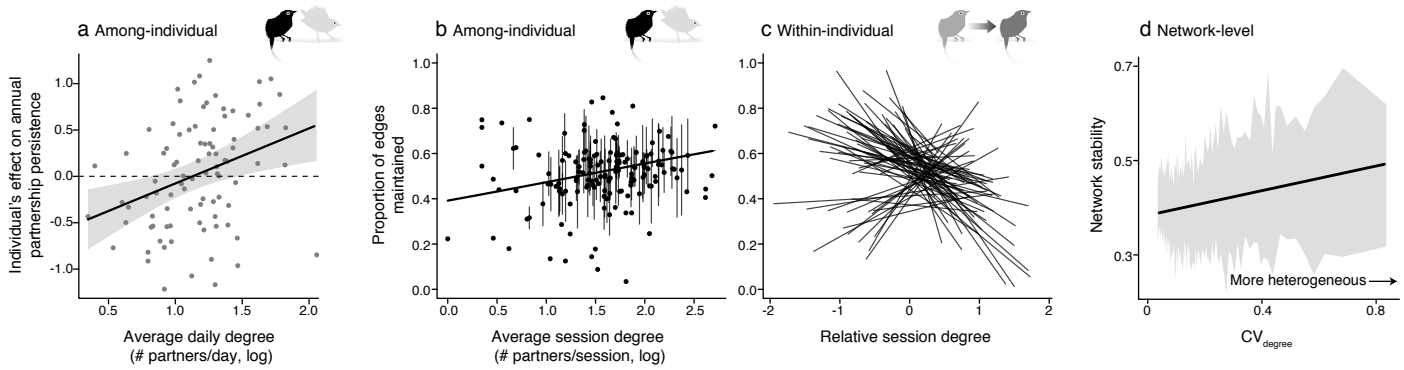

Fig. 4. Behavioral heterogeneity and social stability. Social behavior varies both within and among individuals. a, At the among-individual level, manakins who were consistently more gregarious fostered greater long-term social stability. The plot in a shows how an individual's behavior (x-axis) predicts his effect on annual partnership persistence (y-axis, ±95% confidence interval of the prediction line). Males who consistently interacted with more partners per day (high average daily degree) promoted long-term coalition persistence (n = 90 individuals). b–c, A trade-off is revealed when examining repeated measures within-individuals. The plots in b and c show partial residuals from a variance partitioning analysis of within-season partnership (or edge) maintenance (n = 565 repeated measures of 152 individuals). Despite the positive among-individual effect shown in b, at times when a given male had more partners than his average in c, he was less able to maintain stable partnerships. To visualize among- and within-individual variation, a single average is plotted for each male in b (± SE if a male had >3 measurements), whereas a separate linear fit is shown for individuals with >3 measurements in c. d, Social networks with greater among-individual behavioral heterogeneity (CVdegree) were also more temporally stable in an individual-based simulation. The y-axis shows partial residuals from an analysis that also accounts for the effects of network size, weight, and density (n = 3,000). Shading indicates the 95% central range for partial residuals binned along the x-axis.

Extended Data Fig. 1

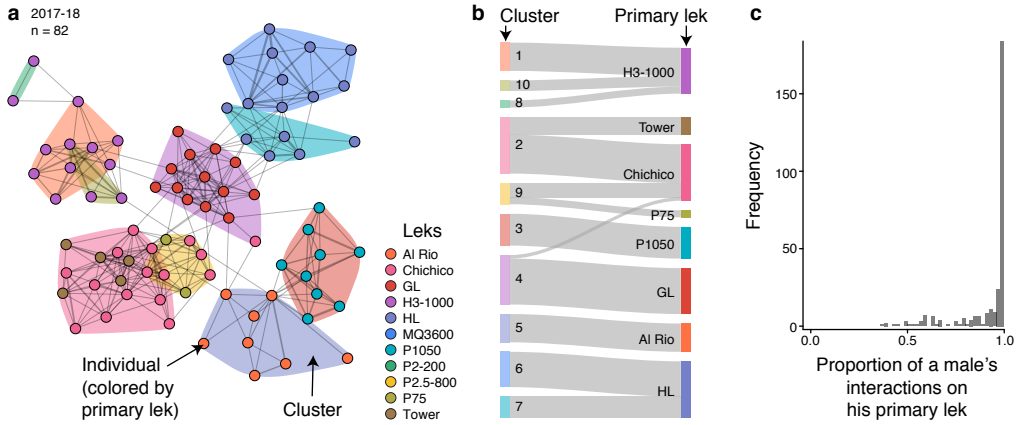

Extended Data Figure 1 | Social structure corresponds to lek structure. We performed a clustering analysis to verify that the lek units captured the natural social structure of the manakin population. The first step was to find the natural community structure of each annual social network (i.e., defined as the aggregation of all recording sessions and all leks in a given field season). To do this, we used the random walk clustering algorithm in the igraph package. The three annual social networks were highly modular (modularity coefficients of 0.70, 0.73, and 0.83, respectively), demonstrating strong clustering of interactions into communities. a, Example annual social network from 2017-18. Each node represents an individual male and is colored according to his primary lek, defined as the site where he engaged in the most cooperative interactions. The overlaid color polygons indicate cluster membership. The layout of the network was determined using the force-directed LGL algorithm, with edges weighted by the interaction frequencies. Next, we compared annual cluster membership to each male's primary lek designation, defined as the lek where the male engaged in the greatest number of social interactions that year. The probability that a male's primary lek matched the majority of his cluster was 90% (266/296 male-years). b, Example Sankey diagram to compare the clustering algorithm with primary lek usage. The relatively low proportion of crossings demonstrates strong correspondence. c, Histogram showing how males typically limited nearly all of their interactions to a single lek. This spatial patterning of interactions creates structure (modularity) in the network, resulting in the strong correspondence between lek structure and the clustering algorithm. Note that the same color schemes are used throughout a–b. Finally, the assortativity coefficient provides another way to compare lek and cluster structure in the social networks. The three annual networks were highly assorted by primary lek (coefficients 0.51, 0.51, and 0.69) to a level that was statistically indistinguishable from the assortment based on cluster membership (coefficients 0.47, 0.52, and 0.69, respectively). Based on this strong correspondence between lek structure and the structure revealed by the clustering algorithm, we conclude that our sampling design was well-matched to the inherent social structure of the population.

Extended Data Fig. 2

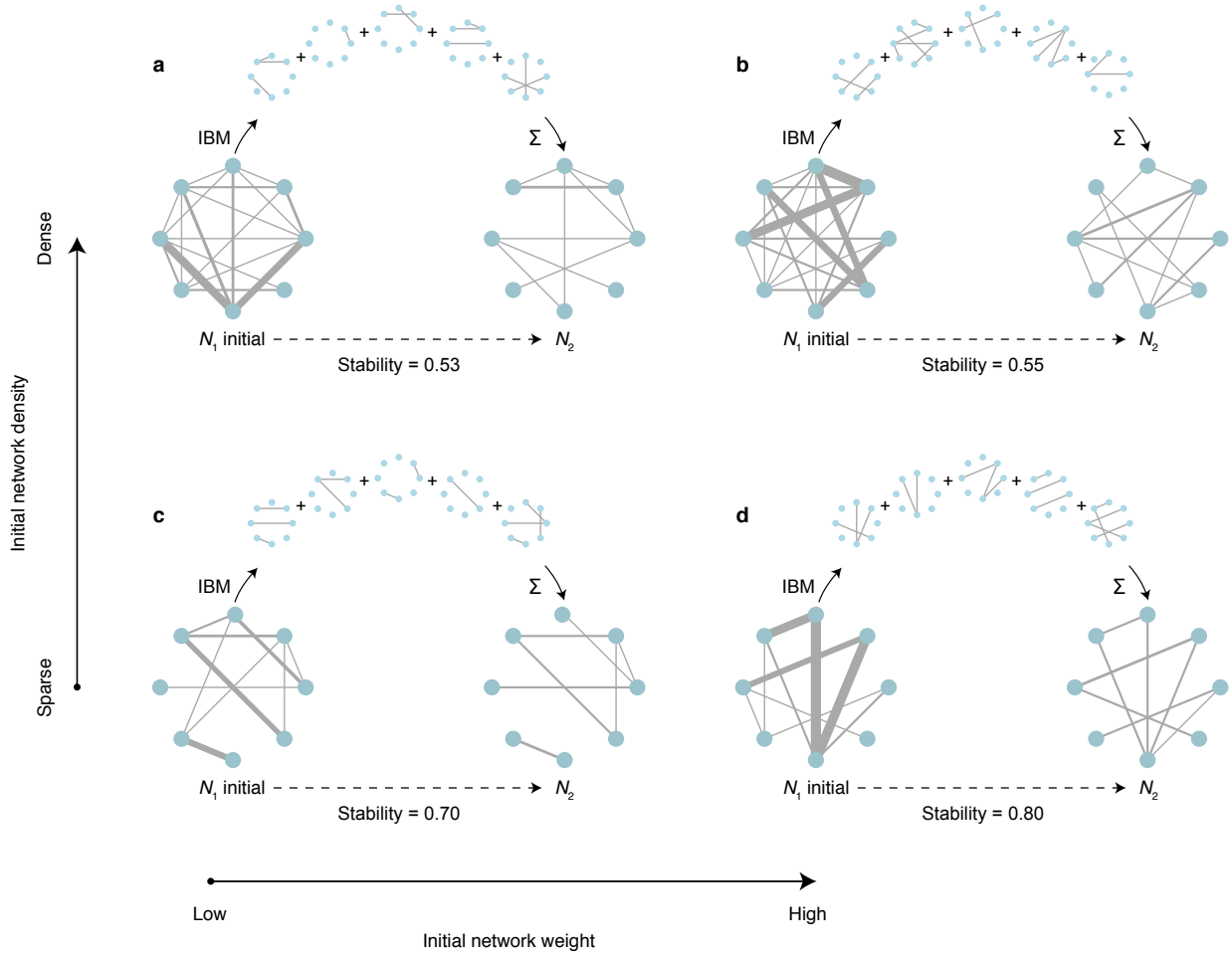

Extended Data Figure 2 | Procedure for the individual-based simulation models. a–d, Four examples illustrate the general approach and the data generated. The initial social network (N1) represents the starting point used to determine the probabilities of subsequent social interactions. Each individual-based model (IBM) was run for five time-steps, akin to measuring interactions across multiple days. During this time, new partnerships were formed, as shown. The subsequent network (N2) represents the sum of new interactions that occurred during the IBM time-steps. The stability score is calculated by comparing the topology of N2 with that of N1. Note that within each example a–d, the layout of particular nodes is kept constant throughout. Edge thicknesses are scaled to the log-transformed interaction frequency in a consistent manner throughout the figure. Note that the N2 networks have a lower network weight as compared to N1, because the time interval for the simulation was relatively short (albeit sufficient to develop a wide range of network stability values). The four examples a–d were chosen because they vary in the initial network weight (increasing left to right) and density (increasing bottom to top). The network size of eight was used in this figure for visual clarity in the illustration; however, in the actual simulations, network sizes ranged from 11-20 individuals.